L^2 Convergent Pixel-Driven Discretizations of Projection Operators

Kristian Bredies and Richard Huber

IGDK 1754

IGDK Colloquium
November 19, 2019 – Augsburg

Project

P 8: Parameter estimation for the Bloch equation from linear projection data and applications in MR fingerprinting (K. Bredies, M. Fornasier)

Member of the IGDK

since 06/2018

Publications

- M. Holler, R. Huber, and F. Knoll.
  Coupled regularization with multiple data discrepancies
  Inverse problems, Volume 34, Number 8, 2018.
- R. Huber, G. Haberfehlner, M. Holler, G. Kothleitner and K. Bredies
  Total Generalized Variation regularization for multi-modal electron tomography
  RCS Nanoscale Volume 11, 5617-5632, 2019
- S. Almi, M. Fornasier, R. Huber
  Data-driven Evolutions of Critical Points
  Under peer review in: SIAM Journal on Mathematics of Data Science, 2019
- K. Bredies, R. Huber
  Convergence Analysis of Pixel-Driven Radon and Fanbeam Transforms
  In preparation to submit in: SIAM Journal on Numerical Analysis, 2019-2020

Tomography in a nutshell

Tomography in a nutshell

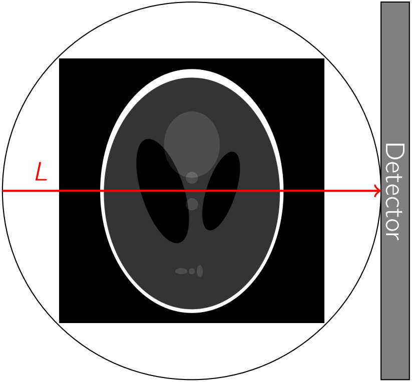

$$\int_L f(x)\,\mathrm{d}\mathcal{H}^1(x)$$

Tomography in a nutshell

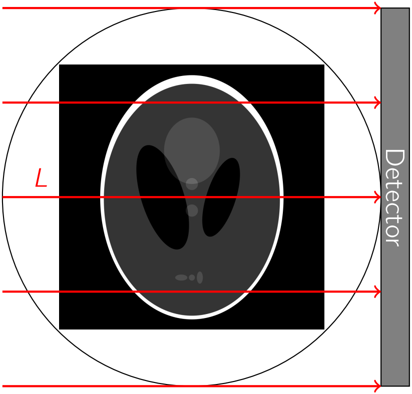

$$\int_L f(x)\,\mathrm{d}\mathcal{H}^1(x)$$

Tomography in a nutshell

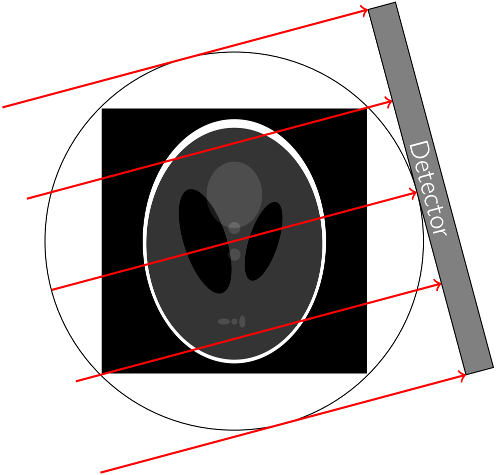

$$\int_L f(x)\,\mathrm{d}\mathcal{H}^1(x)$$

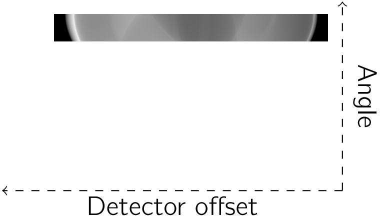

Tomography in a nutshell

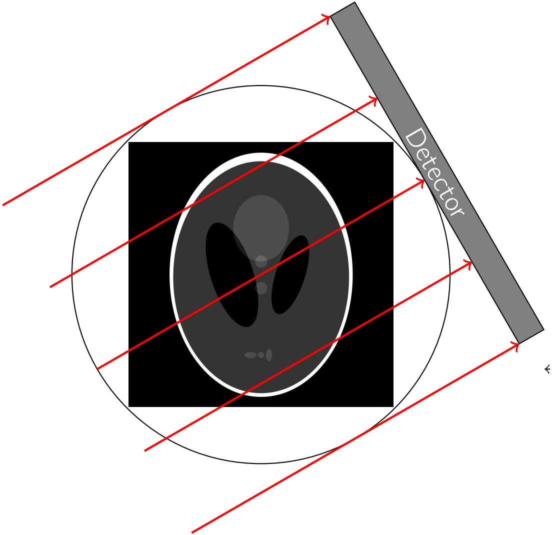

$$\int_L f(x)\,\mathrm{d}\mathcal{H}^1(x)$$

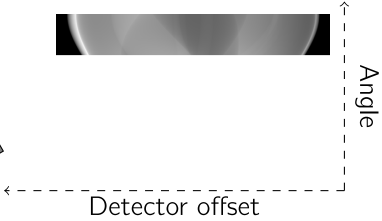

Tomography in a nutshell

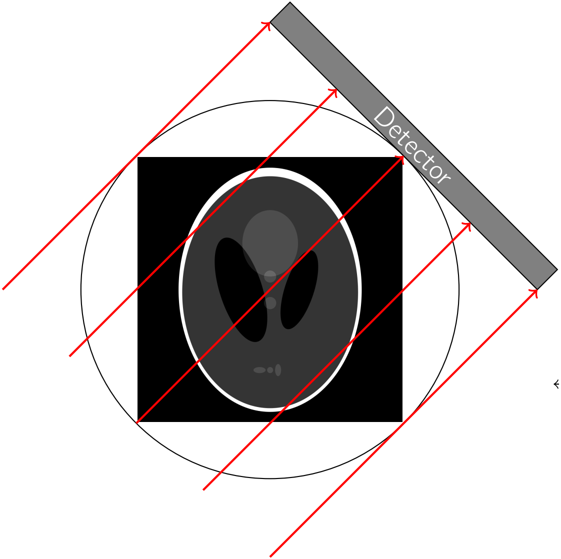

$$\int_L f(x)\,\mathrm{d}\mathcal{H}^1(x)$$

Tomography in a nutshell

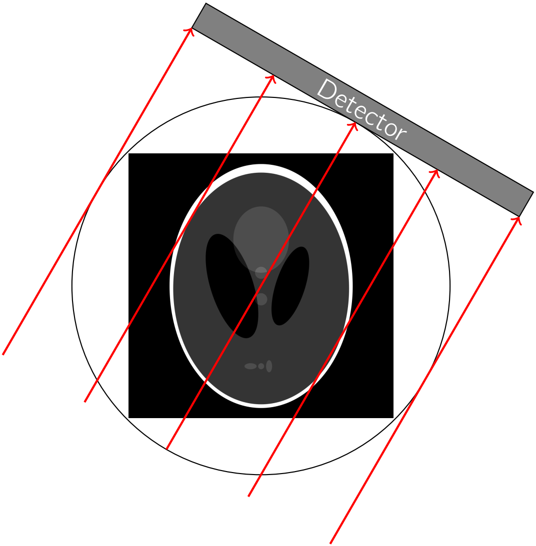

$$\int_L f(x)\,\mathrm{d}\mathcal{H}^1(x)$$

Tomography in a nutshell

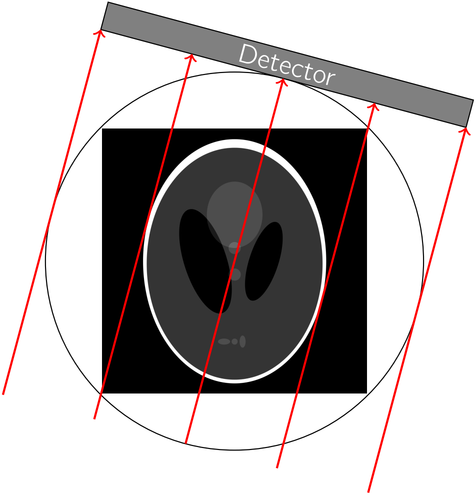

$$\int_L f(x)\,\mathrm{d}\mathcal{H}^1(x)$$

Tomography in a nutshell

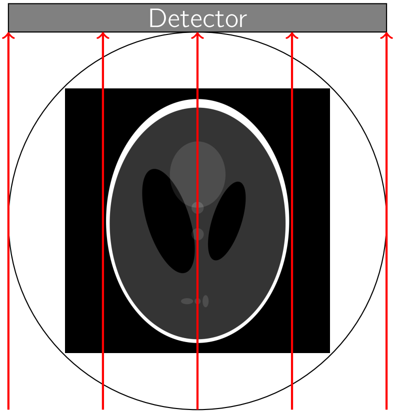

$$\int_L f(x)\,\mathrm{d}\mathcal{H}^1(x)$$

Tomography in a nutshell

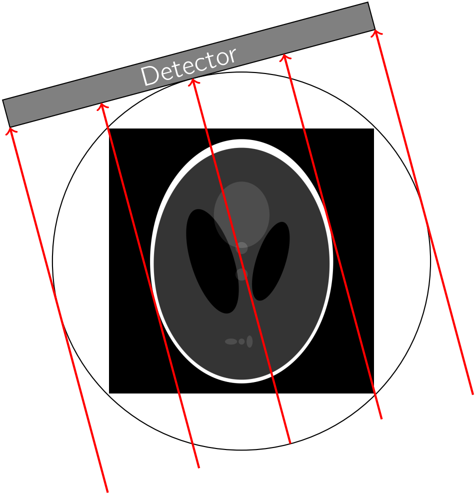

$$\int_L f(x)\,\mathrm{d}\mathcal{H}^1(x)$$

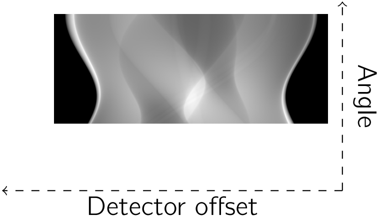

Tomography in a nutshell

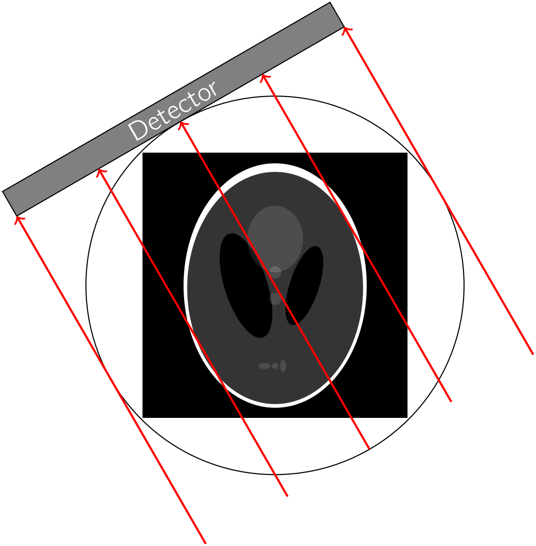

$$\int_L f(x)\,\mathrm{d}\mathcal{H}^1(x)$$

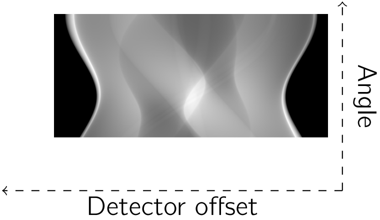

Tomography in a nutshell

$$\int_L f(x)\,\mathrm{d}\mathcal{H}^1(x)$$

Tomography in a nutshell

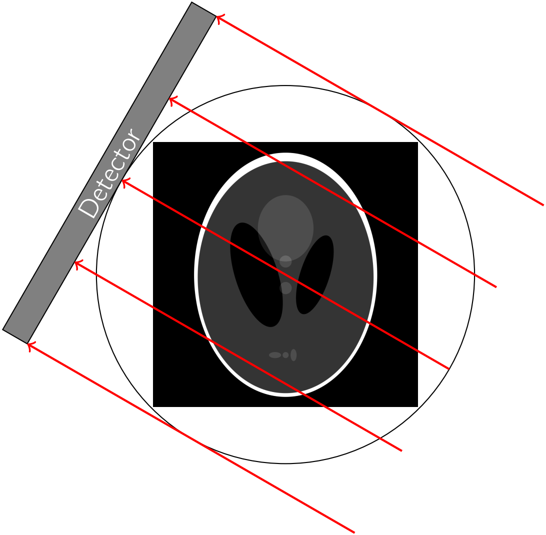

$$\int_L f(x)\,\mathrm{d}\mathcal{H}^1(x)$$

Tomography in a nutshell

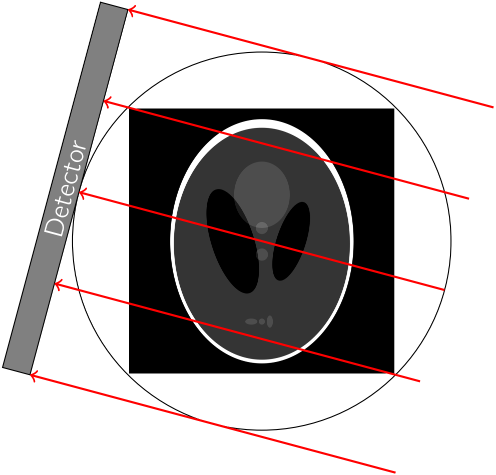

$$\int_L f(x)\, \mathrm{d}\mathcal{H}^1(x)$$

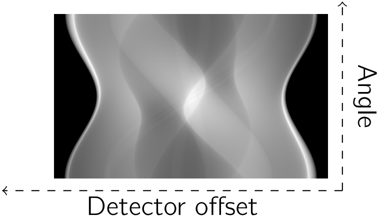

Tomography in a nutshell

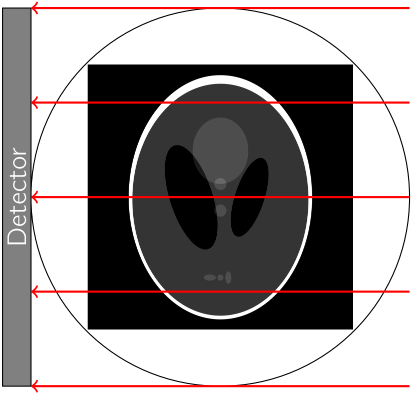

$$\mathcal{R}f = g$$

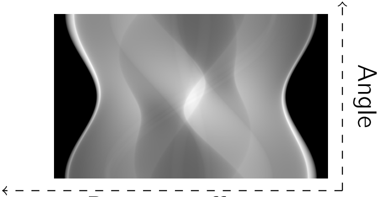

Tomography in a nutshell

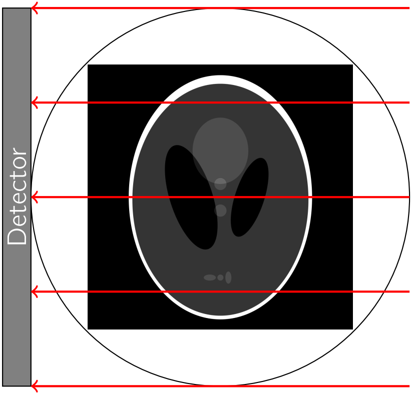

$$\mathcal{R}f = g$$

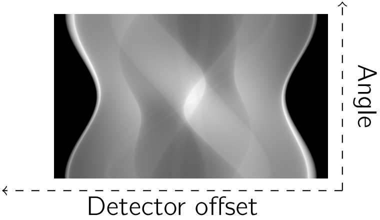

- g ... loss of energy

Tomography in a nutshell

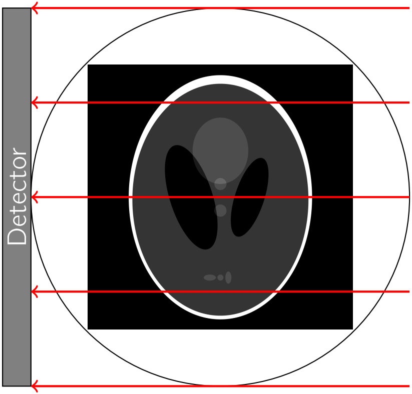

$$\mathcal{R}f = g$$

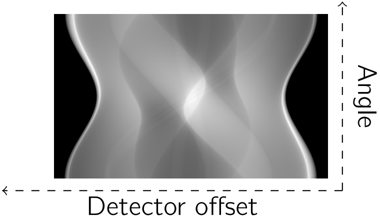

- g ... loss of energy
- f ... unknown density

Tomography in a nutshell

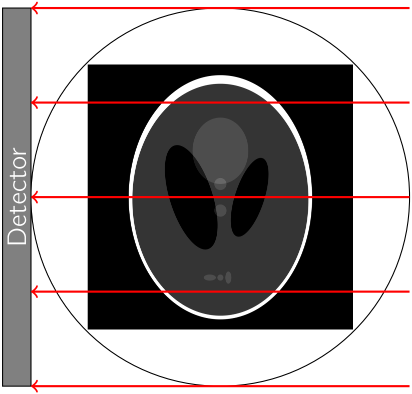

$$\mathcal{R}f = g$$

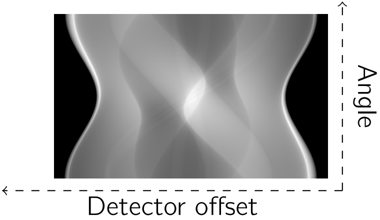

- g ... loss of energy
- f ... unknown density
- $\mathcal{R}$ ... Radon transform

Introduction

- Radon transform $\mathcal{R}$ has various applications in imaging:

Introduction

- Radon transform $\mathcal{R}$ has various applications in imaging:
  - Computed tomography
  - Positron emission tomography,
  - MRI/MRF with radial sampling.

Introduction

- Radon transform $\mathcal{R}$ has various applications in imaging:
  - Computed tomography
  - Positron emission tomography,
  - MRI/MRF with radial sampling.
- Inverse problems (tomographic reconstruction).

Introduction

- Radon transform $\mathcal{R}$ has various applications in imaging:
  - Computed tomography
  - Positron emission tomography,
  - MRI/MRF with radial sampling.
- Inverse problems (tomographic reconstruction).
  - Approaches require $\mathcal{R}$ and $\mathcal{R}^*$,

Introduction

- Radon transform $\mathcal{R}$ has various applications in imaging:
  - Computed tomography
  - Positron emission tomography,
  - MRI/MRF with radial sampling.
- Inverse problems (tomographic reconstruction).
  - Approaches require $\mathcal{R}$ and $\mathcal{R}^*$,
  - Discrete $A \approx \mathcal{R}$ and $B \approx \mathcal{R}^*$,

Introduction

- Radon transform $\mathcal{R}$ has various applications in imaging:
  - Computed tomography
  - Positron emission tomography,
  - MRI/MRF with radial sampling.
- Inverse problems (tomographic reconstruction).
  - Approaches require $\mathcal{R}$ and $\mathcal{R}^*$,
  - Discrete $A \approx \mathcal{R}$ and $B \approx \mathcal{R}^*$,
  - Often $A^* \neq B$.

Introduction

- Radon transform $\mathcal{R}$ has various applications in imaging:
  - Computed tomography
  - Positron emission tomography,
  - MRI/MRF with radial sampling.
- Inverse problems (tomographic reconstruction).
  - Approaches require $\mathcal{R}$ and $\mathcal{R}^*$,
  - Discrete $A \approx \mathcal{R}$ and $B \approx \mathcal{R}^*$,
  - Often $A^* \neq B$.
- Pixel-Driven Projections as discretization

Introduction

- Radon transform $\mathcal{R}$ has various applications in imaging:
  - Computed tomography
  - Positron emission tomography,
  - MRI/MRF with radial sampling.
- Inverse problems (tomographic reconstruction).
  - Approaches require $\mathcal{R}$ and $\mathcal{R}^*$,
  - Discrete $A \approx \mathcal{R}$ and $B \approx \mathcal{R}^*$,
  - Often $A^* \neq B$.
- Pixel-Driven Projections as discretization

Introduction

- Radon transform $\mathcal{R}$ has various applications in imaging:
  - Computed tomography
  - Positron emission tomography,
  - MRI/MRF with radial sampling.
- Inverse problems (tomographic reconstruction).
  - Approaches require $\mathcal{R}$ and $\mathcal{R}^*$,
  - Discrete $A \approx \mathcal{R}$ and $B \approx \mathcal{R}^*$,
  - Often $A^* \neq B$.
- Pixel-Driven Projections as discretization
  - $A^* = B$,

Introduction

- Radon transform $\mathcal{R}$ has various applications in imaging:
  - Computed tomography
  - Positron emission tomography,
  - MRI/MRF with radial sampling.
- Inverse problems (tomographic reconstruction).
  - Approaches require $\mathcal{R}$ and $\mathcal{R}^*$,
  - Discrete $A \approx \mathcal{R}$ and $B \approx \mathcal{R}^*$,
  - Often $A^* \neq B$.
- Pixel-Driven Projections as discretization
  - $A^* = B$,
  - Good approximation of $\mathcal{R}^*$,

Introduction

- Radon transform $\mathcal{R}$ has various applications in imaging:
  - Computed tomography
  - Positron emission tomography,
  - MRI/MRF with radial sampling.
- Inverse problems (tomographic reconstruction).
  - Approaches require $\mathcal{R}$ and $\mathcal{R}^*$,
  - Discrete $A \approx \mathcal{R}$ and $B \approx \mathcal{R}^*$,
  - Often $A^* \neq B$.
- Pixel-Driven Projections as discretization
  - $A^* = B$,
  - Good approximation of $\mathcal{R}^*$,
  - Poor approximation of $\mathcal{R}$,

Introduction

- Radon transform $\mathcal{R}$ has various applications in imaging:
  - Computed tomography
  - Positron emission tomography,
  - MRI/MRF with radial sampling.
- Inverse problems (tomographic reconstruction).
  - Approaches require $\mathcal{R}$ and $\mathcal{R}^*$,
  - Discrete $A \approx \mathcal{R}$ and $B \approx \mathcal{R}^*$,
  - Often $A^* \neq B$.
- Pixel-Driven Projections as discretization
  - $A^* = B$,
  - Good approximation of $\mathcal{R}^*$,
  - Poor approximation of $\mathcal{R}$,
  - No proper mathematical analysis.

Introduction

- Radon transform $\mathcal{R}$ has various applications in imaging:
  - Computed tomography
  - Positron emission tomography,
  - MRI/MRF with radial sampling.
- Inverse problems (tomographic reconstruction).
  - Approaches require $\mathcal{R}$ and $\mathcal{R}^*$,
  - Discrete $A \approx \mathcal{R}$ and $B \approx \mathcal{R}^*$,
  - Often $A^* \neq B$.
- Pixel-Driven Projections as discretization
  - $A^* = B$,
  - Good approximation of $\mathcal{R}^*$,
  - Poor approximation of $\mathcal{R}$,
  - No proper mathematical analysis.

Goal: Proper convergence analysis!

Outline

1. The Radon Transform

Outline

1. The Radon Transform

2. Pixel-Driven Projections

Outline

1. The Radon Transform
2. Pixel-Driven Projections
3. Convergence in Operator Norm

Outline

1. The Radon Transform

2. Pixel-Driven Projections

3. Convergence in Operator Norm

The continuous Radon transform

Definition

Let $\Omega = B(0,1) \subset \mathbb{R}^2$ and $\Omega' =]-1,1[\times[-\pi,\pi[$.

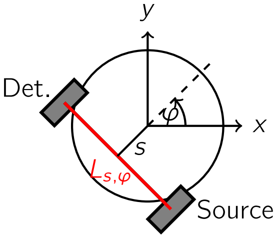

The continuous Radon transform

Definition

Let $\Omega = B(0,1) \subset \mathbb{R}^2$ and $\Omega' =]-1,1[\times [-\pi,\pi[$.

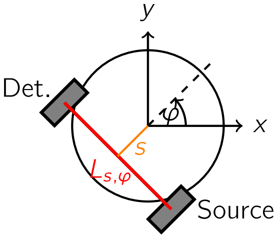

The continuous Radon transform

Definition

Let $\Omega = B(0,1) \subset \mathbb{R}^2$ and $\Omega' =]-1,1[\times [-\pi, \pi[$.

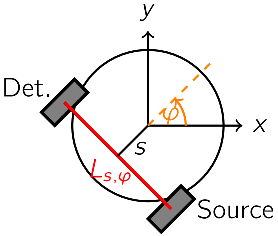

The continuous Radon transform

Definition

Let $\Omega = B(0,1) \subset \mathbb{R}^2$ and $\Omega' =]-1,1[\times[-\pi,\pi[$.
The Radon transform $\mathcal{R}\colon L^2(\Omega) \to L^2(\Omega')$

$$[\mathcal{R}f](s,\varphi) = \int_{L_{s,\varphi}} f(x)\,\mathrm{d}\mathcal{H}^1(x).$$

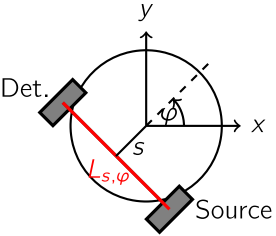

The continuous Radon transform

Definition

Let $\Omega = B(0,1) \subset \mathbb{R}^2$ and $\Omega' =]-1,1[\times[-\pi,\pi[$.
The Radon transform $\mathcal{R}\colon L^2(\Omega) \to L^2(\Omega')$

$$[\mathcal{R}f](s,\varphi) = \int_{L_{s,\varphi}} f(x)\,\mathrm{d}\mathcal{H}^1(x).$$

The backprojection $\mathcal{R}^*\colon L^2(\Omega') \to L^2(\Omega)$

$$[\mathcal{R}^*g](x) = \int_{[-\pi,\pi[} g(x\cdot\vartheta(\varphi),\varphi)\,\mathrm{d}\varphi.$$

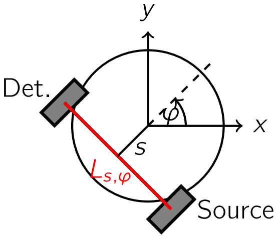

The continuous Radon transform

Definition

Let $\Omega = B(0,1) \subset \mathbb{R}^2$ and $\Omega' =]-1,1[\times[-\pi,\pi[$.
The Radon transform $\mathcal{R}\colon L^2(\Omega) \to L^2(\Omega')$

$$[\mathcal{R}f](s,\varphi) = \int_{L_{s,\varphi}} f(x)\,\mathrm{d}\mathcal{H}^1(x).$$

The backprojection $\mathcal{R}^*\colon L^2(\Omega') \to L^2(\Omega)$

$$[\mathcal{R}^*g](x) = \int_{[-\pi,\pi[} g(x\cdot\vartheta(\varphi),\varphi)\,\mathrm{d}\varphi.$$

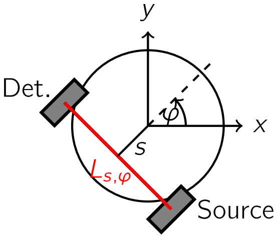

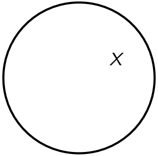

The continuous Radon transform

Definition

Let $\Omega = B(0,1) \subset \mathbb{R}^2$ and $\Omega' =]-1,1[\times[-\pi,\pi[$.
The Radon transform $\mathcal{R}\colon L^2(\Omega) \to L^2(\Omega')$

$$[\mathcal{R}f](s,\varphi) = \int_{L_{s,\varphi}} f(x)\,\mathrm{d}\mathcal{H}^1(x).$$

The backprojection $\mathcal{R}^*\colon L^2(\Omega') \to L^2(\Omega)$

$$[\mathcal{R}^* g](x) = \int_{[-\pi,\pi[} g(x\cdot\vartheta(\varphi),\varphi)\,\mathrm{d}\varphi.$$

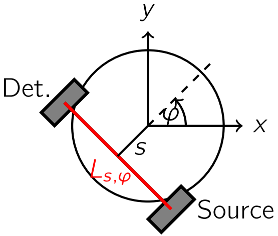

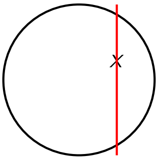

The continuous Radon transform

Definition

Let $\Omega = B(0,1) \subset \mathbb{R}^2$ and $\Omega' =]-1,1[\times[-\pi,\pi[$.
The Radon transform $\mathcal{R}\colon L^2(\Omega) \to L^2(\Omega')$

$$[\mathcal{R}f](s,\varphi) = \int_{L_{s,\varphi}} f(x)\,\mathrm{d}\mathcal{H}^1(x).$$

The backprojection $\mathcal{R}^*\colon L^2(\Omega') \to L^2(\Omega)$

$$[\mathcal{R}^* g](x) = \int_{[-\pi,\pi[} g(x\cdot\vartheta(\varphi),\varphi)\,\mathrm{d}\varphi.$$

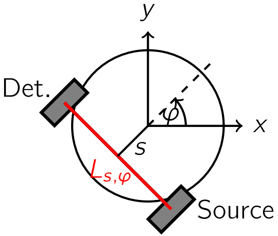

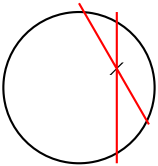

The continuous Radon transform

Definition

Let $\Omega = B(0,1) \subset \mathbb{R}^2$ and $\Omega' =]-1,1[\times[-\pi,\pi[$.
The Radon transform $\mathcal{R}\colon L^2(\Omega) \to L^2(\Omega')$

$$[\mathcal{R}f](s,\varphi) = \int_{L_{s,\varphi}} f(x)\,\mathrm{d}\mathcal{H}^1(x).$$

The backprojection $\mathcal{R}^*\colon L^2(\Omega') \to L^2(\Omega)$

$$[\mathcal{R}^*g](x) = \int_{[-\pi,\pi[} g(x\cdot\vartheta(\varphi),\varphi)\,\mathrm{d}\varphi.$$

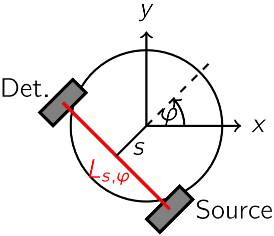

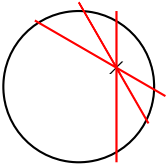

The continuous Radon transform

Definition

Let $\Omega = B(0,1) \subset \mathbb{R}^2$ and $\Omega' =]-1,1[\times[-\pi,\pi[$.
The Radon transform $\mathcal{R}\colon L^2(\Omega) \to L^2(\Omega')$

$$[\mathcal{R}f](s,\varphi) = \int_{L_{s,\varphi}} f(x)\,\mathrm{d}\mathcal{H}^1(x).$$

The backprojection $\mathcal{R}^*\colon L^2(\Omega') \to L^2(\Omega)$

$$[\mathcal{R}^*g](x) = \int_{[-\pi,\pi[} g(x\cdot\vartheta(\varphi),\varphi)\,\mathrm{d}\varphi.$$

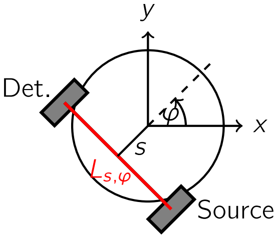

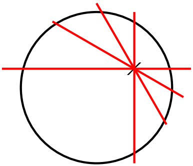

The continuous Radon transform

Definition

Let $\Omega = B(0,1) \subset \mathbb{R}^2$ and $\Omega' =]-1,1[\times[-\pi,\pi[$.
The Radon transform $\mathcal{R}\colon L^2(\Omega) \to L^2(\Omega')$

$$[\mathcal{R}f](s,\varphi) = \int_{L_{s,\varphi}} f(x)\,\mathrm{d}\mathcal{H}^1(x).$$

The backprojection $\mathcal{R}^*\colon L^2(\Omega') \to L^2(\Omega)$

$$[\mathcal{R}^*g](x) = \int_{[-\pi,\pi[} g(x\cdot\vartheta(\varphi),\varphi)\,\mathrm{d}\varphi.$$

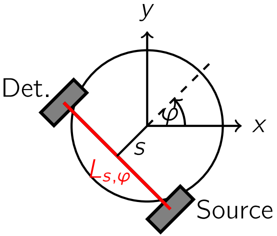

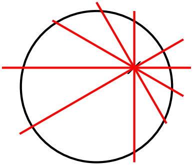

The continuous Radon transform

Definition

Let $\Omega = B(0,1) \subset \mathbb{R}^2$ and $\Omega' =]-1,1[\times[-\pi,\pi[$.
The Radon transform $\mathcal{R}\colon L^2(\Omega) \to L^2(\Omega')$

$$[\mathcal{R}f](s,\varphi) = \int_{L_{s,\varphi}} f(x)\,\mathrm{d}\mathcal{H}^1(x).$$

The backprojection $\mathcal{R}^*\colon L^2(\Omega') \to L^2(\Omega)$

$$[\mathcal{R}^*g](x) = \int_{[-\pi,\pi[} g(x\cdot\vartheta(\varphi),\varphi)\,\mathrm{d}\varphi.$$

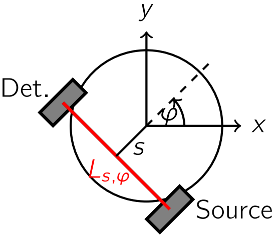

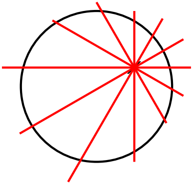

Parallel beam setting

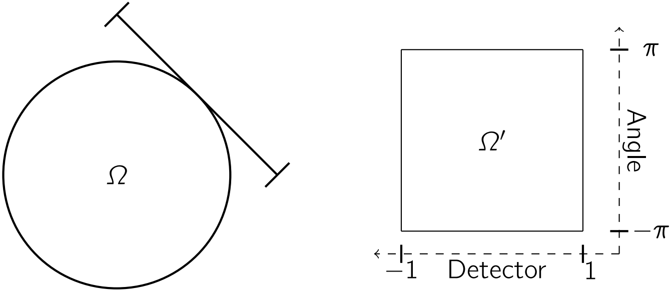

Parallel beam setting

- Angles: $\varphi_1 < \cdots < \varphi_Q$, with $\vartheta_q = (\cos(\varphi_q), \sin(\varphi_q))$, $\Phi_q = [\frac{\varphi_{q-1}+\varphi_q}{2}, \frac{\varphi_q+\varphi_{q+1}}{2}[$ and $\delta_\varphi = \max_q |\Phi_q|$.

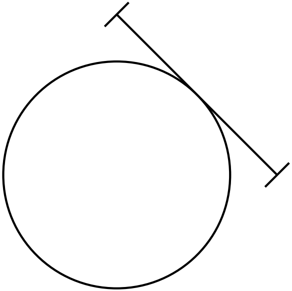

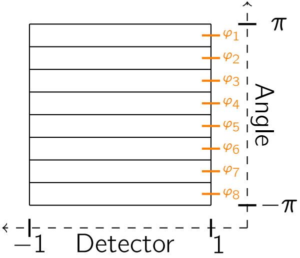

Parallel beam setting

- Angles: $\varphi_1 < \cdots < \varphi_Q$, with $\vartheta_q = (\cos(\varphi_q), \sin(\varphi_q))$, $\Phi_q = [\frac{\varphi_{q-1}+\varphi_q}{2}, \frac{\varphi_q+\varphi_{q+1}}{2}[$ and $\delta_\varphi = \max_q |\Phi_q|$.
- Detector offsets: Equispaced $s_1 < \cdots < s_P$ with corresponding pixels $S_p = s_p + [-\frac{\delta_s}{2}, \frac{\delta_s}{2}[$.

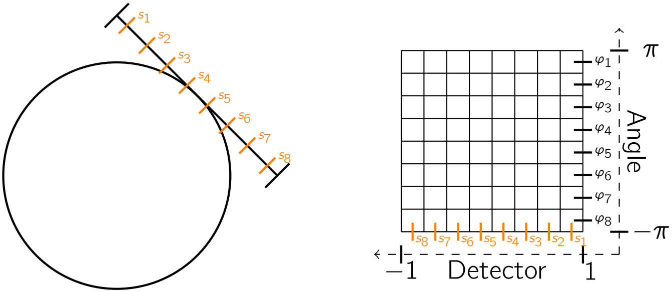

Parallel beam setting

- Angles: $\varphi_1 < \cdots < \varphi_Q$, with $\vartheta_q = (\cos(\varphi_q), \sin(\varphi_q))$, $\Phi_q = [\frac{\varphi_{q-1}+\varphi_q}{2}, \frac{\varphi_q+\varphi_{q+1}}{2}[$ and $\delta_\varphi = \max_q |\Phi_q|$.
- Detector offsets: Equispaced $s_1 < \cdots < s_P$ with corresponding pixels $S_p = s_p + [-\frac{\delta_s}{2}, \frac{\delta_s}{2}[$.

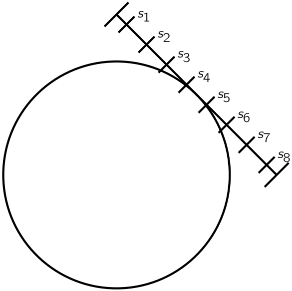

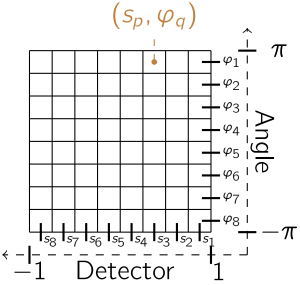

Parallel beam setting

- Angles: $\varphi_1 < \cdots < \varphi_Q$, with $\vartheta_q = (\cos(\varphi_q), \sin(\varphi_q))$, $\Phi_q = [\frac{\varphi_{q-1}+\varphi_q}{2}, \frac{\varphi_q+\varphi_{q+1}}{2}[$ and $\delta_\varphi = \max_q |\Phi_q|$.
- Detector offsets: Equispaced $s_1 < \cdots < s_P$ with corresponding pixels $S_p = s_p + [-\frac{\delta_s}{2}, \frac{\delta_s}{2}[$.

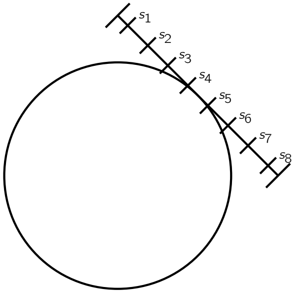

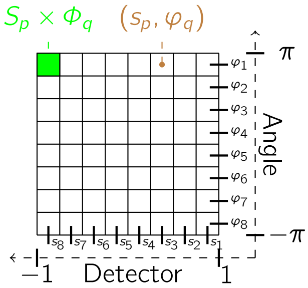

Parallel beam setting

- Angles: $\varphi_1 < \cdots < \varphi_Q$, with $\vartheta_q = (\cos(\varphi_q), \sin(\varphi_q))$, $\Phi_q = [\frac{\varphi_{q-1}+\varphi_q}{2}, \frac{\varphi_q+\varphi_{q+1}}{2}[$ and $\delta_\varphi = \max_q |\Phi_q|$.
- Detector offsets: Equispaced $s_1 < \cdots < s_P$ with corresponding pixels $S_p = s_p + [-\frac{\delta_s}{2}, \frac{\delta_s}{2}[$.
- Image pixels: Equispaced pixels X_{ij} with centers x_{ij} and width δ_x.

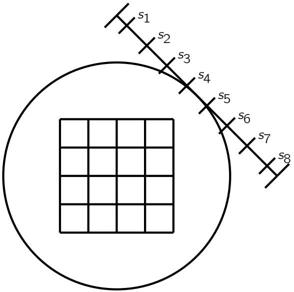

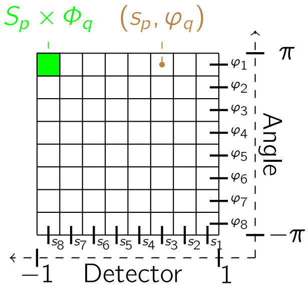

Parallel beam setting

- Angles: $\varphi_1 < \cdots < \varphi_Q$, with $\vartheta_q = (\cos(\varphi_q), \sin(\varphi_q))$, $\Phi_q = [\frac{\varphi_{q-1}+\varphi_q}{2}, \frac{\varphi_q+\varphi_{q+1}}{2}[$ and $\delta_\varphi = \max_q |\Phi_q|$.
- Detector offsets: Equispaced $s_1 < \cdots < s_P$ with corresponding pixels $S_p = s_p + [-\frac{\delta_s}{2}, \frac{\delta_s}{2}[$.
- Image pixels: Equispaced pixels X_{ij} with centers x_{ij} and width δ_x.

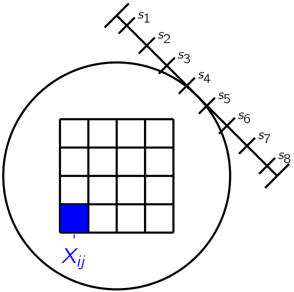

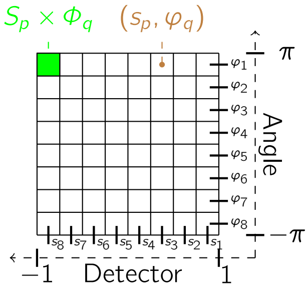

Parallel beam setting

- Angles: $\varphi_1 < \cdots < \varphi_Q$, with $\vartheta_q = (\cos(\varphi_q), \sin(\varphi_q))$, $\Phi_q = [\frac{\varphi_{q-1}+\varphi_q}{2}, \frac{\varphi_q+\varphi_{q+1}}{2}[$ and $\delta_\varphi = \max_q |\Phi_q|$.
- Detector offsets: Equispaced $s_1 < \cdots < s_P$ with corresponding pixels $S_p = s_p + [-\frac{\delta_s}{2}, \frac{\delta_s}{2}[$.
- Image pixels: Equispaced pixels X_{ij} with centers x_{ij} and width δ_x.

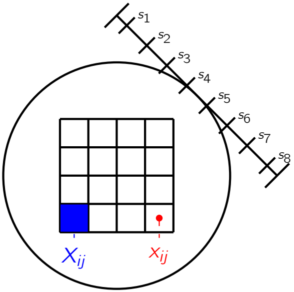

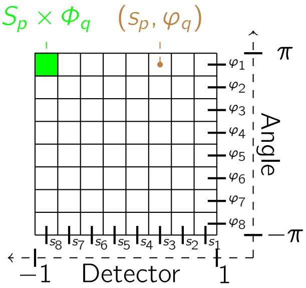

Parallel beam setting

- Angles: $\varphi_1 < \cdots < \varphi_Q$, with $\vartheta_q = (\cos(\varphi_q), \sin(\varphi_q))$, $\Phi_q = [\frac{\varphi_{q-1}+\varphi_q}{2}, \frac{\varphi_q+\varphi_{q+1}}{2}[$ and $\delta_\varphi = \max_q |\Phi_q|$.
- Detector offsets: Equispaced $s_1 < \cdots < s_P$ with corresponding pixels $S_p = s_p + [-\frac{\delta_s}{2}, \frac{\delta_s}{2}[$.
- Image pixels: Equispaced pixels X_{ij} with centers x_{ij} and width δ_x.
- Discretization parameters: δ_s, δ_φ and δ_x.

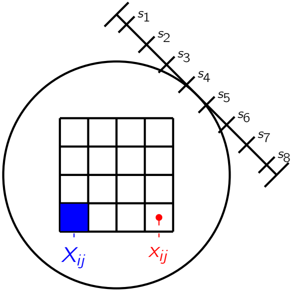

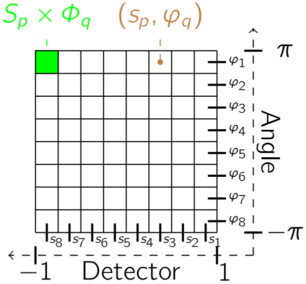

Outline

1. The Radon Transform

2. Pixel-Driven Projections

3. Convergence in Operator Norm

Pixel-driven approach

$$[\mathcal{R}^* g](x_{ij}) = \int_{[-\pi,\pi[} g(x_{ij} \cdot \vartheta(\varphi), \varphi)\,\mathrm{d}\varphi$$

Pixel-driven approach

$$[\mathcal{R}^* g](x_{ij}) = \int_{[-\pi,\pi[} g(x_{ij} \cdot \vartheta(\varphi), \varphi) \,\mathrm{d}\varphi \approx \sum_q |\Phi_q| g(x_{ij} \cdot \vartheta_q, \varphi_q)$$

Pixel-driven approach

$$[\mathcal{R}^* g](x_{ij}) = \int_{[-\pi,\pi[} g(x_{ij} \cdot \vartheta(\varphi), \varphi) \,\mathrm{d}\varphi \approx \sum_q |\Phi_q| g(x_{ij} \cdot \vartheta_q, \varphi_q)$$

$$\approx \sum_q \frac{|\Phi_q|}{\delta_s} \sum_{p: |x_{ij} \cdot \vartheta_q - s_p| \leq \delta_s} (\delta_s - |x_{ij} \cdot \vartheta_q - s_p|) g(s_p, \varphi_q)$$

Pixel-driven approach

$$[\mathcal{R}^* g](x_{ij}) = \int_{[-\pi,\pi[} g(x_{ij} \cdot \vartheta(\varphi), \varphi)\, \mathrm{d}\varphi \approx \sum_q |\Phi_q| g(x_{ij} \cdot \vartheta_q, \varphi_q)$$

$$\approx \sum_q \frac{|\Phi_q|}{\delta_s} \sum_{p: |x_{ij}\cdot\vartheta_q - s_p| \leq \delta_s} (\delta_s - |x_{ij} \cdot \vartheta_q - s_p|) g(s_p, \varphi_q) := [(\mathcal{R}^{\mathrm{PD}})^* g]_{ij}$$

Pixel-driven approach

$$[\mathcal{R}^* g](x_{ij}) = \int_{[-\pi,\pi[} g(x_{ij} \cdot \vartheta(\varphi), \varphi)\, \mathrm{d}\varphi \approx \sum_q |\Phi_q| g(x_{ij} \cdot \vartheta_q, \varphi_q)$$

$$\approx \sum_q \frac{|\Phi_q|}{\delta_s} \sum_{p : |x_{ij} \cdot \vartheta_q - s_p| \leq \delta_s} (\delta_s - |x_{ij} \cdot \vartheta_q - s_p|) g(s_p, \varphi_q) := [(\mathcal{R}^{\mathrm{PD}})^* g]_{ij}$$

$$[\mathcal{R}^{\mathrm{PD}} f]_{pq} := \frac{1}{\delta_s} \sum_{ij : |x_{ij} \cdot \vartheta_q - s_p| \leq \delta_s} (\delta_s - |s_p - x_{ij} \cdot \vartheta_q|) f_{ij},$$

Pixel-driven approach

$$[\mathcal{R}^* g](x_{ij}) = \int_{[-\pi,\pi[} g(x_{ij} \cdot \vartheta(\varphi), \varphi) \, \mathrm{d}\varphi \approx \sum_q |\Phi_q| g(x_{ij} \cdot \vartheta_q, \varphi_q)$$

$$\approx \sum_q \frac{|\Phi_q|}{\delta_s} \sum_{p : |x_{ij} \cdot \vartheta_q - s_p| \leq \delta_s} (\delta_s - |x_{ij} \cdot \vartheta_q - s_p|) g(s_p, \varphi_q) := [(\mathcal{R}^{\mathrm{PD}})^* g]_{ij}$$

$$[\mathcal{R}^{\mathrm{PD}} f]_{pq} := \frac{1}{\delta_s} \sum_{ij : |x_{ij} \cdot \vartheta_q - s_p| \leq \delta_s} (\delta_s - |s_p - x_{ij} \cdot \vartheta_q|) f_{ij},$$

- Computation only considers distance to lines.

Pixel-driven approach

$$[\mathcal{R}^* g](x_{ij}) = \int_{[-\pi,\pi[} g(x_{ij} \cdot \vartheta(\varphi), \varphi) \, \mathrm{d}\varphi \approx \sum_q |\Phi_q| g(x_{ij} \cdot \vartheta_q, \varphi_q)$$

$$\approx \sum_q \frac{|\Phi_q|}{\delta_s} \sum_{p : |x_{ij} \cdot \vartheta_q - s_p| \leq \delta_s} (\delta_s - |x_{ij} \cdot \vartheta_q - s_p|) g(s_p, \varphi_q) := [(\mathcal{R}^{\mathrm{PD}})^* g]_{ij}$$

$$[\mathcal{R}^{\mathrm{PD}} f]_{pq} := \frac{1}{\delta_s} \sum_{ij : |x_{ij} \cdot \vartheta_q - s_p| \leq \delta_s} (\delta_s - |s_p - x_{ij} \cdot \vartheta_q|) f_{ij},$$

- Computation only considers distance to lines.
- Unclear if proper discretization.

Pixel-driven approach

$$[\mathcal{R}^* g](x_{ij}) = \int_{[-\pi,\pi[} g(x_{ij}\cdot\vartheta(\varphi),\varphi)\,\mathrm{d}\varphi \approx \sum_q |\Phi_q| g(x_{ij}\cdot\vartheta_q,\varphi_q)$$

$$\approx \sum_q \frac{|\Phi_q|}{\delta_s} \sum_{p:|x_{ij}\cdot\vartheta_q - s_p|\leq\delta_s} (\delta_s - |x_{ij}\cdot\vartheta_q - s_p|) g(s_p,\varphi_q) := [(\mathcal{R}^{\mathrm{PD}})^* g]_{ij}$$

$$[\mathcal{R}^{\mathrm{PD}} f]_{pq} := \frac{1}{\delta_s} \sum_{ij:|x_{ij}\cdot\vartheta_q - s_p|\leq\delta_s} (\delta_s - |s_p - x_{ij}\cdot\vartheta_q|) f_{ij},$$

- Computation only considers distance to lines.
- Unclear if proper discretization.
- Known to create oscillations.

Approximation with area integrals

$\mathcal{H}^1 \llcorner L_{s,\varphi} \approx W_{s,\varphi}(x) = \frac{1}{\delta_s^2} w_{\delta_s}(x \cdot \vartheta(\varphi) - s)\mathcal{L}^2(x)$ where $w_{\delta_s}(t) = \max(0, \delta_s - |t|)$.

Approximation with area integrals

$\mathcal{H}^1 \llcorner L_{s,\varphi} \approx W_{s,\varphi}(x) = \frac{1}{\delta_s^2} w_{\delta_s}(x \cdot \vartheta(\varphi) - s)\mathcal{L}^2(x)$ where $w_{\delta_s}(t) = \max(0, \delta_s - |t|)$.

Definition

$$[\mathcal{R}_\delta f](s,\varphi) := \int_\Omega f(x)\,\mathrm{d}W_{s,\varphi}(x)$$

Approximation with area integrals

$\mathcal{H}^1 \llcorner L_{s,\varphi} \approx W_{s,\varphi}(x) = \frac{1}{\delta_s^2} w_{\delta_s}(x \cdot \vartheta(\varphi) - s)\mathcal{L}^2(x)$ where $w_{\delta_s}(t) = \max(0, \delta_s - |t|)$.

Definition

$$[\mathcal{R}_\delta f](s,\varphi) := \int_\Omega f(x)\, \mathrm{d}W_{s,\varphi}(x) = \frac{1}{\delta_s^2} \int_{\mathbb{R}} w_{\delta_s}(s-t)\mathcal{R}f(t,\varphi)\, \mathrm{d}t$$

Approximation with area integrals

$\mathcal{H}^1 \llcorner L_{s,\varphi} \approx W_{s,\varphi}(x) = \frac{1}{\delta_s^2} w_{\delta_s}(x \cdot \vartheta(\varphi) - s)\mathcal{L}^2(x)$ where $w_{\delta_s}(t) = \max(0, \delta_s - |t|)$.

Definition

$$[\mathcal{R}_\delta f](s,\varphi) := \int_\Omega f(x)\,\mathrm{d}W_{s,\varphi}(x) = \frac{1}{\delta_s^2}\int_{\mathbb{R}} w_{\delta_s}(s-t)\mathcal{R}f(t,\varphi)\,\mathrm{d}t$$

With $f_{\delta_x} = \sum_{ij} f_{ij}\delta_{x_{ij}}$ with $f_{ij} = \int_{X_{ij}} f(x)\,\mathrm{d}x$

$$[\mathcal{R}_\delta f_{\delta_x}](s_p,\varphi_q) = \sum_{ij} f_{ij} w_{\delta_s}(x_{ij}\cdot\vartheta(\varphi_q) - s_p) = [\mathcal{R}^{\mathrm{PD}} f]_{pq}.$$

Approximation with area integrals

$\mathcal{H}^1 \llcorner L_{s,\varphi} \approx W_{s,\varphi}(x) = \frac{1}{\delta_s^2} w_{\delta_s}(x \cdot \vartheta(\varphi) - s)\mathcal{L}^2(x)$ where $w_{\delta_s}(t) = \max(0, \delta_s - |t|)$.

Definition

$$[\mathcal{R}_\delta f](s,\varphi) := \int_\Omega f(x)\,\mathrm{d}W_{s,\varphi}(x) = \frac{1}{\delta_s^2}\int_{\mathbb{R}} w_{\delta_s}(s-t)\mathcal{R}f(t,\varphi)\,\mathrm{d}t$$

With $f_{\delta_x} = \sum_{ij} f_{ij}\delta_{x_{ij}}$ with $f_{ij} = \int_{X_{ij}} f(x)\,\mathrm{d}x$

$$[\mathcal{R}_\delta f_{\delta_x}](s_p,\varphi_q) = \sum_{ij} f_{ij} w_{\delta_s}(x_{ij}\cdot\vartheta(\varphi_q) - s_p) = [\mathcal{R}^{\mathrm{PD}} f]_{pq}.$$

Definition (Continuous Pixel-Driven Radon Transform)

$$\mathcal{R}^{\delta_x}_{\delta_s,\delta_\varphi} : L^2(\Omega) \to L^2(\Omega')$$

Approximation with area integrals

$\mathcal{H}^1 \llcorner L_{s,\varphi} \approx W_{s,\varphi}(x) = \frac{1}{\delta_s^2} w_{\delta_s}(x \cdot \vartheta(\varphi) - s)\mathcal{L}^2(x)$ where $w_{\delta_s}(t) = \max(0, \delta_s - |t|)$.

Definition

$$[\mathcal{R}_\delta f](s,\varphi) := \int_\Omega f(x)\,\mathrm{d}W_{s,\varphi}(x) = \frac{1}{\delta_s^2}\int_{\mathbb{R}} w_{\delta_s}(s-t)\mathcal{R}f(t,\varphi)\,\mathrm{d}t$$

With $f_{\delta_x} = \sum_{ij} f_{ij}\delta_{x_{ij}}$ with $f_{ij} = \int_{X_{ij}} f(x)\,\mathrm{d}x$

$$[\mathcal{R}_\delta f_{\delta_x}](s_p,\varphi_q) = \sum_{ij} f_{ij} w_{\delta_s}(x_{ij}\cdot\vartheta(\varphi_q) - s_p) = [\mathcal{R}^{\mathrm{PD}} f]_{pq}.$$

Definition (Continuous Pixel-Driven Radon Transform)

$$\mathcal{R}^{\delta_x}_{\delta_s,\delta_\varphi} : L^2(\Omega) \to L^2(\Omega')$$

$$\mathcal{R}^{\delta_x}_{\delta_s,\delta_\varphi} f(s,\varphi) = [\mathcal{R}_\delta f_{\delta_x}](s_p,\varphi_q) \qquad \forall s \in S_p, \varphi \in \Phi_q$$

Modelling perspective

$$[\mathcal{R}_\delta f](s,\varphi) = \overbrace{\frac{1}{\delta_s^2}\int_{\mathbb{R}} w_{\delta_s}(s-t)\mathcal{R}f(t,\varphi)\,\mathrm{d}t}$$

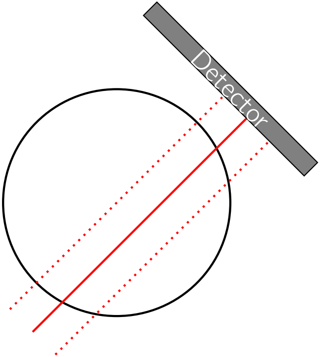

Modelling perspective

$$[\mathcal{R}_\delta f](s,\varphi) = \overbrace{\frac{1}{\delta_s^2}\int_{\mathbb{R}} w_{\delta_s}(s-t)\mathcal{R}f(t,\varphi)\,\mathrm{d}t}$$

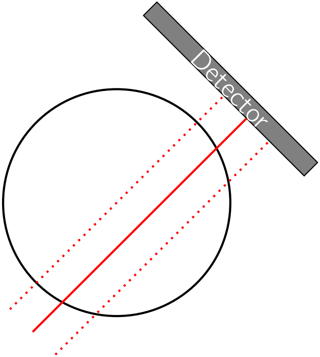

- Pixels detect lines from range of offsets.

Modelling perspective

$$[\mathcal{R}_\delta f](s,\varphi) = \overbrace{\frac{1}{\delta_s^2}\int_{\mathbb{R}} w_{\delta_s}(s-t)\mathcal{R}f(t,\varphi)\,\mathrm{d}t}^{\text{Averaging}}$$

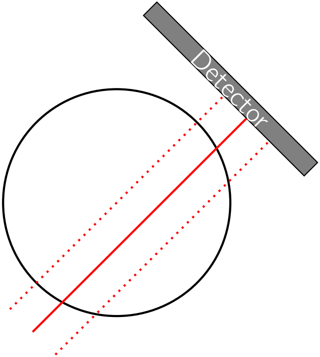

- Pixels detect lines from range of offsets.
- Averaging of the Radon transform.

Modelling perspective

$$[\mathcal{R}_\delta f](s,\varphi) = \overbrace{\frac{1}{\delta_s^2}\int_{\mathbb{R}} w_{\delta_s}(s-t)\mathcal{R}f(t,\varphi)\,\mathrm{d}t}^{\text{Averaging}}$$

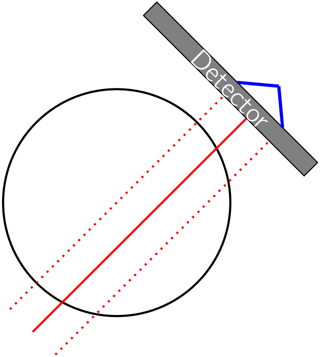

- Pixels detect lines from range of offsets.
- Averaging of the Radon transform.
- Hat shaped sensitivity field.

Modelling perspective

$$[\mathcal{R}_\delta f](s,\varphi) = \overbrace{\frac{1}{\delta_s^2}\int_{\mathbb{R}} w_{\delta_s}(s-t)\mathcal{R}f(t,\varphi)\,\mathrm{d}t}^{\text{Averaging}}$$
$$= \underbrace{\frac{1}{\delta_s^2}\int_{\Omega} w_{\delta_s}(x\cdot\vartheta(\varphi)-s)f(x)\,\mathrm{d}x}$$

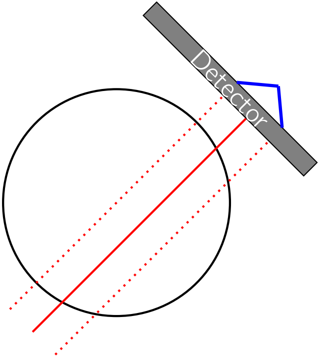

- Pixels detect lines from range of offsets.
- Averaging of the Radon transform.
- Hat shaped sensitivity field.
- Weighted area integral.

Modelling perspective

$$[\mathcal{R}_\delta f](s,\varphi) = \overbrace{\frac{1}{\delta_s^2}\int_{\mathbb{R}} w_{\delta_s}(s-t)\mathcal{R}f(t,\varphi)\,\mathrm{d}t}^{\text{Averaging}}$$

$$= \underbrace{\frac{1}{\delta_s^2}\int_{\Omega} w_{\delta_s}(x\cdot\vartheta(\varphi)-s)f(x)\,\mathrm{d}x}_{\text{Hat shaped sensitivity,}}$$

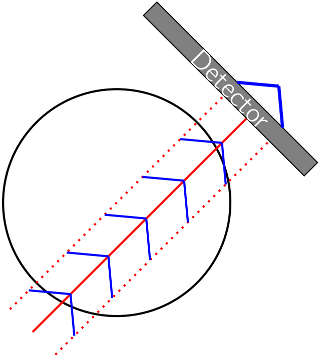

- Pixels detect lines from range of offsets.
- Averaging of the Radon transform.
- Hat shaped sensitivity field.
- Weighted area integral.
- Hat shaped contribution to rays.

Outline

1. The Radon Transform
2. Pixel-Driven Projections
3. Convergence in Operator Norm

Regularity of Radon transform

Definition (L^2 Modulus of Continuity)

For $g \in L^2(\Omega')$ the modulus of continuity is

Regularity of Radon transform

Definition (L^2 Modulus of Continuity)

For $g \in L^2(\Omega')$ the modulus of continuity is

$$M_g(h,\gamma) = \|T_{h,\gamma} g - g\|_{L^2} = \sqrt{\int_{\Omega'} |g(s+h,\varphi+\gamma) - g(s,\varphi)|^2 \,\mathrm{d}(s,\varphi)}.$$

Regularity of Radon transform

Definition (L^2 Modulus of Continuity)

For $g \in L^2(\Omega')$ the modulus of continuity is

$$M_g(h,\gamma) = \| T_{h,\gamma} g - g\|_{L^2} = \sqrt{\int_{\Omega'} |g(s+h,\varphi+\gamma) - g(s,\varphi)|^2 \,\mathrm{d}(s,\varphi)}.$$

Note that $\lim_{|(h,\gamma)|\to 0} \frac{M_g(h,\gamma)^2}{(|h|^2+|\gamma|^2)^{1+\alpha}} < \infty$ corresponds to regularity statements.

Regularity of Radon transform

Definition (L^2 Modulus of Continuity)

For $g \in L^2(\Omega')$ the modulus of continuity is

$$M_g(h,\gamma) = \|T_{h,\gamma} g - g\|_{L^2} = \sqrt{\int_{\Omega'} |g(s+h,\varphi+\gamma) - g(s,\varphi)|^2 \,\mathrm{d}(s,\varphi)}.$$

Note that $\lim_{|(h,\gamma)|\to 0} \frac{M_g(h,\gamma)^2}{(|h|^2+|\gamma|^2)^{1+\alpha}} < \infty$ corresponds to regularity statements.

Lemma

For $f \in L^2(\Omega)$ and $g = \mathcal{R} f$ we have $M_g(h,0) \leq c\sqrt{|h|}\|f\|$.

Regularity of Radon transform

Definition (L^2 Modulus of Continuity)

For $g \in L^2(\Omega')$ the modulus of continuity is

$$M_g(h,\gamma) = \|T_{h,\gamma} g - g\|_{L^2} = \sqrt{\int_{\Omega'} |g(s+h,\varphi+\gamma) - g(s,\varphi)|^2 \,\mathrm{d}(s,\varphi)}.$$

Note that $\lim_{|(h,\gamma)|\to 0} \frac{M_g(h,\gamma)^2}{(|h|^2+|\gamma|^2)^{1+\alpha}} < \infty$ corresponds to regularity statements.

Lemma

For $f \in L^2(\Omega)$ and $g = \mathcal{R}f$ we have $M_g(h,0) \leq c\sqrt{|h|}\|f\|$.

Convergence statement

Theorem

Let $\delta_s \to 0$, $\frac{\delta_x}{\delta_s} \to 0$ *and* $\frac{\delta_\varphi}{\delta_s} \to 0$. *Then*

$$\|\mathcal{R}_{\delta_s,\delta_\varphi}^{\delta_x} - \mathcal{R}\| \to 0 \qquad \text{and} \qquad \|(\mathcal{R}_{\delta_s,\delta_\varphi}^{\delta_x})^* - \mathcal{R}^*\| \to 0.$$

Convergence statement

Theorem

Let $\delta_s \to 0$, $\frac{\delta_x}{\delta_s} \to 0$ *and* $\frac{\delta_\varphi}{\delta_s} \to 0$. *Then*

$$\|\mathcal{R}^{\delta_x}_{\delta_s,\delta_\varphi} - \mathcal{R}\| \to 0 \qquad \text{and} \qquad \|(\mathcal{R}^{\delta_x}_{\delta_s,\delta_\varphi})^* - \mathcal{R}^*\| \to 0.$$

If additionally $\frac{\delta_x}{\delta_s} = \mathcal{O}(\delta_s^\epsilon)$ *and* $\frac{\delta_\varphi}{\delta_s} = \mathcal{O}(\delta_s^\epsilon)$ *for some* $\epsilon \in [0, \frac{1}{2}]$, *then*

$$\|\mathcal{R}^{\delta_x}_{\delta_s,\delta_\varphi} - \mathcal{R}\| = \mathcal{O}(\delta_s^\epsilon) \qquad \text{and} \qquad \|(\mathcal{R}^{\delta_x}_{\delta_s,\delta_\varphi})^* - \mathcal{R}^*\| = \mathcal{O}(\delta_s^\epsilon).$$

Convergence statement

Theorem

Let $\delta_s \to 0$, $\frac{\delta_x}{\delta_s} \to 0$ *and* $\frac{\delta_\varphi}{\delta_s} \to 0$. *Then*

$$\|\mathcal{R}^{\delta_x}_{\delta_s,\delta_\varphi} - \mathcal{R}\| \to 0 \qquad \text{and} \qquad \|(\mathcal{R}^{\delta_x}_{\delta_s,\delta_\varphi})^* - \mathcal{R}^*\| \to 0.$$

If additionally $\frac{\delta_x}{\delta_s} = \mathcal{O}(\delta_s^\epsilon)$ *and* $\frac{\delta_\varphi}{\delta_s} = \mathcal{O}(\delta_s^\epsilon)$ *for some* $\epsilon \in [0, \frac{1}{2}]$, *then*

$$\|\mathcal{R}^{\delta_x}_{\delta_s,\delta_\varphi} - \mathcal{R}\| = \mathcal{O}(\delta_s^\epsilon) \qquad \text{and} \qquad \|(\mathcal{R}^{\delta_x}_{\delta_s,\delta_\varphi})^* - \mathcal{R}^*\| = \mathcal{O}(\delta_s^\epsilon).$$

If moreover $M_{\mathcal{R}f}(\delta_s, 0) = \mathcal{O}(\delta_s^\epsilon)$ *or* $M_g(\delta_s, 0) = \mathcal{O}(\delta_s^\epsilon)$, *then*

$$\|\mathcal{R}^{\delta_x}_{\delta_s,\delta_\varphi} f - \mathcal{R}f\| = \mathcal{O}(\delta_s^\epsilon) \qquad \text{and} \qquad \|(\mathcal{R}^{\delta_x}_{\delta_s,\delta_\varphi})^* g - \mathcal{R}^* g\| = \mathcal{O}(\delta_s^\epsilon)$$

without the restriction $\epsilon \leq \frac{1}{2}$.

Proof.

$$\|\mathcal{R}^{\delta_x}_{\delta_s,\delta_\varphi} - \mathcal{R}\| \leq \underbrace{\|\mathcal{R}^{\delta_x}_{\delta_s,\delta_\varphi} - \mathcal{R}_{\delta_s,\delta_\varphi}\|} + \underbrace{\|\mathcal{R}_{\delta_s,\delta_\varphi} - \mathcal{R}_{\delta_s}\|} + \underbrace{\|\mathcal{R}_{\delta_s} - \mathcal{R}\|}.$$

□

Proof.

$$\|\mathcal{R}^{\delta_x}_{\delta_s,\delta_\varphi} - \mathcal{R}\| \leq \underbrace{\|\mathcal{R}^{\delta_x}_{\delta_s,\delta_\varphi} - \mathcal{R}_{\delta_s,\delta_\varphi}\|}_{\leq c\frac{\delta_x}{\delta_s}} + \underbrace{\|\mathcal{R}_{\delta_s,\delta_\varphi} - \mathcal{R}_{\delta_s}\|}_{\leq c\frac{\delta_\varphi}{\delta_s}} + \underbrace{\|\mathcal{R}_{\delta_s} - \mathcal{R}\|}_{\leq c\sqrt{\delta_s}}.$$

□

Proof.

$$\|\mathcal{R}^{\delta_x}_{\delta_s,\delta_\varphi} - \mathcal{R}\| \leq \underbrace{\|\mathcal{R}^{\delta_x}_{\delta_s,\delta_\varphi} - \mathcal{R}_{\delta_s,\delta_\varphi}\|}_{\leq c\frac{\delta_x}{\delta_s}} + \underbrace{\|\mathcal{R}_{\delta_s,\delta_\varphi} - \mathcal{R}_{\delta_s}\|}_{\leq c\frac{\delta_\varphi}{\delta_s}} + \underbrace{\|\mathcal{R}_{\delta_s} - \mathcal{R}\|}_{\leq c\sqrt{\delta_s}}.$$

- For $\delta_s \to 0$, $\frac{\delta_x}{\delta_s} \to 0$ and $\frac{\delta_\varphi}{\delta_s} \to 0$ this yields convergence in operator norm.

□

Proof.

$$\|\mathcal{R}^{\delta_x}_{\delta_s,\delta_\varphi} - \mathcal{R}\| \leq \underbrace{\|\mathcal{R}^{\delta_x}_{\delta_s,\delta_\varphi} - \mathcal{R}_{\delta_s,\delta_\varphi}\|}_{\leq c\frac{\delta_x}{\delta_s}} + \underbrace{\|\mathcal{R}_{\delta_s,\delta_\varphi} - \mathcal{R}_{\delta_s}\|}_{\leq c\frac{\delta_\varphi}{\delta_s}} + \underbrace{\|\mathcal{R}_{\delta_s} - \mathcal{R}\|}_{\leq c\sqrt{\delta_s}}.$$

- For $\delta_s \to 0$, $\frac{\delta_x}{\delta_s} \to 0$ and $\frac{\delta_\varphi}{\delta_s} \to 0$ this yields convergence in operator norm.
- For $\frac{\delta_x}{\delta_s} = \mathcal{O}(\delta_s^\epsilon)$ and $\frac{\delta_\varphi}{\delta_s} = \mathcal{O}(\delta_s^\epsilon)$ the rates follow.

□

Proof.

$$\|\mathcal{R}^{\delta_x}_{\delta_s,\delta_\varphi} - \mathcal{R}\| \leq \underbrace{\|\mathcal{R}^{\delta_x}_{\delta_s,\delta_\varphi} - \mathcal{R}_{\delta_s,\delta_\varphi}\|}_{\leq c\frac{\delta_x}{\delta_s}} + \underbrace{\|\mathcal{R}_{\delta_s,\delta_\varphi} - \mathcal{R}_{\delta_s}\|}_{\leq c\frac{\delta_\varphi}{\delta_s}} + \underbrace{\|\mathcal{R}_{\delta_s} - \mathcal{R}\|}_{\leq c\sqrt{\delta_s}}.$$

- For $\delta_s \to 0$, $\frac{\delta_x}{\delta_s} \to 0$ and $\frac{\delta_\varphi}{\delta_s} \to 0$ this yields convergence in operator norm.
- For $\frac{\delta_x}{\delta_s} = \mathcal{O}(\delta_s^\epsilon)$ and $\frac{\delta_\varphi}{\delta_s} = \mathcal{O}(\delta_s^\epsilon)$ the rates follow.
- In case of higher regularity $\|\mathcal{R}_{\delta_s} f - \mathcal{R} f\|$ or $\|(\mathcal{R}_{\delta_s})^* g - \mathcal{R}^* g\|$ converges at higher rates.

□

Proof.

$$\|\mathcal{R}^{\delta_x}_{\delta_s,\delta_\varphi} - \mathcal{R}\| \leq \underbrace{\|\mathcal{R}^{\delta_x}_{\delta_s,\delta_\varphi} - \mathcal{R}_{\delta_s,\delta_\varphi}\|}_{\leq c\frac{\delta_x}{\delta_s}} + \underbrace{\|\mathcal{R}_{\delta_s,\delta_\varphi} - \mathcal{R}_{\delta_s}\|}_{\leq c\frac{\delta_\varphi}{\delta_s}} + \underbrace{\|\mathcal{R}_{\delta_s} - \mathcal{R}\|}_{\leq c\sqrt{\delta_s}}.$$

- For $\delta_s \to 0$, $\frac{\delta_x}{\delta_s} \to 0$ and $\frac{\delta_\varphi}{\delta_s} \to 0$ this yields convergence in operator norm.
- For $\frac{\delta_x}{\delta_s} = \mathcal{O}(\delta_s^\epsilon)$ and $\frac{\delta_\varphi}{\delta_s} = \mathcal{O}(\delta_s^\epsilon)$ the rates follow.
- In case of higher regularity $\|\mathcal{R}_{\delta_s} f - \mathcal{R} f\|$ or $\|(\mathcal{R}_{\delta_s})^* g - \mathcal{R}^* g\|$ converges at higher rates.

□

Remark

- We required $\frac{\delta_x}{\delta_s} \to 0$.
- Standard $\delta_x \approx \delta_s$ not justified.

Conclusion

- Discretization of the Radon transform:
  - Approximation with area integral,
  - Dirac peaks in pixel centers,
  - Extrapolation from sinogram pixel centers.

Conclusion

- Discretization of the Radon transform:
  - Approximation with area integral,
  - Dirac peaks in pixel centers,
  - Extrapolation from sinogram pixel centers.
- Convergence:
  - Suitable discretization parameter $\delta_s \to 0$, $\frac{\delta_x}{\delta_s} \to 0$ and $\frac{\delta_\varphi}{\delta_s} \to 0$,
  - Convergence in operator norm,
  - Rates for $\frac{\delta_x}{\delta_s} = \mathcal{O}(\delta_s^\epsilon)$ and $\frac{\delta_\varphi}{\delta_s} = \mathcal{O}(\delta_s^\epsilon)$.

Conclusion

- Discretization of the Radon transform:
  - Approximation with area integral,
  - Dirac peaks in pixel centers,
  - Extrapolation from sinogram pixel centers.
- Convergence:
  - Suitable discretization parameter $\delta_s \to 0$, $\frac{\delta_x}{\delta_s} \to 0$ and $\frac{\delta_\varphi}{\delta_s} \to 0$,
  - Convergence in operator norm,
  - Rates for $\frac{\delta_x}{\delta_s} = \mathcal{O}(\delta_s^\epsilon)$ and $\frac{\delta_\varphi}{\delta_s} = \mathcal{O}(\delta_s^\epsilon)$.
- Related work:
  - Sparse angle Radon transform,
  - Fanbeam transform,

Conclusion

- Discretization of the Radon transform:
  - Approximation with area integral,
  - Dirac peaks in pixel centers,
  - Extrapolation from sinogram pixel centers.
- Convergence:
  - Suitable discretization parameter $\delta_s \to 0$, $\frac{\delta_x}{\delta_s} \to 0$ and $\frac{\delta_\varphi}{\delta_s} \to 0$,
  - Convergence in operator norm,
  - Rates for $\frac{\delta_x}{\delta_s} = \mathcal{O}(\delta_s^\epsilon)$ and $\frac{\delta_\varphi}{\delta_s} = \mathcal{O}(\delta_s^\epsilon)$.
- Related work:
  - Sparse angle Radon transform,
  - Fanbeam transform,
- Outlook:
  - Conebeam transformation of 3D Radon transform,
  - Extend convergence analysis.